Early-Time Exponential Instabilities in Nonchaotic Quantum Systems

Efim B. Rozenbaum,[1,2,*] Leonid A. Bunimovich,[3] and Victor Galitski[1,2]
[1]Joint Quantum Institute, University of Maryland, College Park, Maryland 20742, USA
[2]Condensed Matter Theory Center, Department of Physics, University of Maryland, College Park, Maryland 20742, USA
[3]School of Mathematics, Georgia Institute of Technology, Atlanta, Georgia 30332, USA

(Received 24 September 2019; accepted 1 June 2020; published 1 July 2020)

The majority of classical dynamical systems are chaotic and exhibit the butterfly effect: a minute change in initial conditions has exponentially large effects later on. But this phenomenon is difficult to reconcile with quantum mechanics. One of the main goals in the field of quantum chaos is to establish a correspondence between the dynamics of classical chaotic systems and their quantum counterparts. In isolated systems in the absence of decoherence, there is such a correspondence in dynamics, but it usually persists only over a short time window, after which quantum interference washes out classical chaos. We demonstrate that quantum mechanics can also play the opposite role and generate exponential instabilities in classically nonchaotic systems within this early-time window. Our calculations employ the out-of-time-ordered correlator (OTOC)—a diagnostic that reduces to the Lyapunov exponent in the classical limit but is well defined for general quantum systems. We show that certain classically nonchaotic models, such as polygonal billiards, demonstrate a Lyapunov-like exponential growth of the OTOC at early times with Planck's-constant-dependent rates. This behavior is sharply contrasted with the slow early-time growth of the analog of the OTOC in the systems' classical counterparts. These results suggest that classical-to-quantum correspondence in dynamics is violated in the OTOC even before quantum interference develops.

DOI: 10.1103/PhysRevLett.125.014101

Introduction.—Quantum mechanics generally washes out sharp features of classical dynamics due to its wavelike nature and the uncertainty principle. It becomes crucial for chaotic systems because sharp features such as sensitive dependence on initial conditions—the butterfly effect—are eventually destroyed. In isolated systems, the butterfly effect is suppressed after a short period of semiclassical evolution. The scrambling or Ehrenfest time t_E grows logarithmically with system size [1–4].

Even though the Ehrenfest time is usually short even in macroscopic isolated systems, decoherence can reset dynamics back to the semiclassical regime. This explains why classical chaotic dynamics is ubiquitously observed [3–6] (for alternative views on the long Ehrenfest-time "paradox," see Ref. [7]). Regardless of the explanation, the behavior of quantum systems in the Ehrenfest window and the fate of classical-to-quantum correspondence in this regime are of fundamental interest, and we focus on this regime in the present Letter. In particular, we demonstrate here that quantum mechanics can induce short-time exponential instabilities in models, which are classically nonchaotic. While our construction is specific to billiards, we believe that this behavior ubiquitously exists in a variety of dynamical systems.

We start with a simple set of observations. Consider a classical "mathematical billiard," i.e., a point particle within a closed domain reflecting off of its hard walls, such as the polygonal black shape in Fig. 1. It has been rigorously proven [8] that the Kolmogorov–Sinai (KS) entropy and the closely related Lyapunov exponents of *any* polygonal billiard are strictly zero. Next, consider the corresponding "physical billiard," a classical hard disk of radius r_p reflecting off of the same polygonal walls. This physical billiard is equivalent to a mathematical billiard of a smaller size, since the particle's center is not allowed to approach

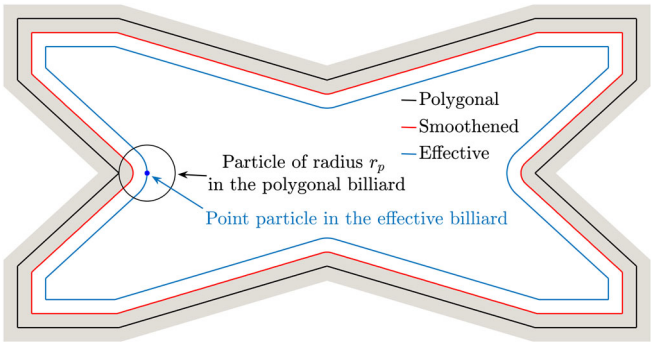

FIG. 1. Outer black line: a polygonal butterfly-shaped billiard. Inner blue line: effective mathematical billiard hosting a point particle equivalent to the outer polygonal billiard hosting a solid disk of radius r_p. The inward-pointing corners of the billiard are rounded into circular arcs or radius r_p, making the effective mathematical billiard classically chaotic with positive Lyapunov exponent. Gray shaded region: a close sub-r_p vicinity of the billiard wall. Middle red line: a smoothened billiard used for comparison below.

the walls closer than r_p. This equivalent billiard is shown by the inner blue shape in Fig. 1. We assume that the particle's mass is concentrated in its center and ignore rotational motion. A crucial observation [9] is that this redrawing gives rise to a smoothing of sharp features of nonconvex polygons. The resulting shape is no longer a polygon, and the obstruction for the KS entropy to vanish is removed. Indeed, the inner blue billiard in Fig. 1 is classically chaotic, with a positive Lyapunov exponent. Finally, consider a quantum particle in a nonconvex polygonal billiard. Semiclassical early-time dynamics of a quantum wave packet is in some sense similar to motion of a finite-size classical particle, i.e., classically chaotic motion in the physical billiard. As shown below, there indeed exist exponential instabilities in classically nonchaotic systems such as this one, hence providing an example of violation of the conventional view on the classical-to-quantum correspondence.

To diagnose this behavior, we employ the out-of-time-ordered correlator (OTOC). It was introduced in Ref. [10] and used recently in the pioneering works by Kitaev [11] and Maldacena *et al.* [12] to define and describe many-body quantum chaos. In the last few years, the OTOC has become a popular tool to describe "quantum chaos" in a variety of systems (see, e.g., Ref. [13]). It was shown in Refs. [14–16] that the exponential growth of the OTOC, although not always equal, might be connected to the exponential divergences of orbits in the phase space of an effective classical system. In certain cases, such as the celebrated Sinai billiard [17] and Bunimovich stadium [18], it is straightforward to understand this classical limit. Below, we consider nonchaotic polygonal billiards instead. In a polygon, for any pair of trajectories—no matter how close the initial conditions are—one can identify the origin of each trajectory evolving the dynamics backward in time [8], ensuring that the KS entropy is zero. Note that in the ergodic hierarchy, which, in the order of "increasing chaoticity" consists of the following systems:

$$\boxed{\text{Ergodic}} \supset \boxed{\begin{matrix}\text{Weakly}\\ \text{Mixing (WM)}\end{matrix}} \supset \boxed{\begin{matrix}\text{Strongly}\\ \text{Mixing (SM)}\end{matrix}} \supset \boxed{\begin{matrix}\text{Kolmogorov}\\ \text{(K-)}\end{matrix}} \supset \boxed{\begin{matrix}\text{Bernoulli}\\ \text{(B-)}\end{matrix}},$$

The polygonal billiards fall within, at most, the SM class. Only the K- and B- systems are chaotic and have a positive KS entropy (see, e.g., Ref. [19] for a detailed discussion of the hierarchy). Interestingly, however, the mixing property at the classical level can be sufficient to generate Wigner–Dyson or intermediate energy level statistics on the quantum side, as was shown, for example, in Ref. [20] for a family of irrational triangular billiards [21].

Apart from this "quantum" Lyapunov instability, where quantum mechanics effectively promotes the corresponding classical system in the ergodic hierarchy, there are potentially more prosaic sources of early-time instabilities in OTOC. First, note that the classical definition of exponential Lyapunov instabilities involves taking two limits: infinitesimally small initial separation in the phase space and infinite time limit in the subsequent evolution. However, neither limit is available quantum mechanically because a wave packet always has a finite size per uncertainty principle and subsequently spreads out on timescales of order the Ehrenfest time. Second, there is a distinction between the quantum-mechanical expectation value in the way quasiclassical trajectories are accounted for and the classical phase-space average [14]. Therefore, in most numerical simulations of OTOCs, the proper Lyapunov limit cannot be enforced and the dynamics of the wave packets may involve spurious rapid growth. To explore these types of phenomena, we also study convex polygonal billiards (specifically an irrational triangle).

Models.—We perform explicit calculations for the billiard shown in Fig. 1, a quadrilateral nonconvex billiard, and a triangular billiard defined below.

We launch a wave packet with the initial wave function

$$\Psi_0(\mathbf{r}) \propto \exp\left[-\frac{(\mathbf{r}-\mathbf{r}_0)^2}{2\hbar_{\text{eff}}\sigma^2} + \frac{i}{\hbar_{\text{eff}}}\mathbf{p}_0\cdot\mathbf{r}\right] \tag{1}$$

by decomposing it into the billiard's energy eigenstates and evolving accordingly (see Fig. 2, which illustrates a representative time evolution). This requires numerical solution of the Schrödinger equation for the billiard:

$$-\frac{\hbar_{\text{eff}}^2}{2}\nabla^2\Psi(\mathbf{r}) = E\Psi(\mathbf{r}), \qquad \Psi(\mathbf{r})|_{\mathbf{r}\in\text{billiard walls}} = 0. \tag{2}$$

Here $\hbar_{\text{eff}} = \hbar/(p_0\sqrt{A})$, $A = 1$ is the billiard's area, and $p_0 = |\mathbf{p}_0| = 1$ is the wave packet's average momentum. We also set the particle's mass $m = 1$. The butterfly-shaped billiard has two reflection symmetries: $x \to -x$ and $y \to -y$. Thus, its eigenstates fall into four parity classes. To enforce this symmetry and speed up the calculations, we solve the eigenvalue problem on a quarter of the billiard, imposing the Dirichlet and/or Neumann boundary conditions on each cut, which defines a parity class.

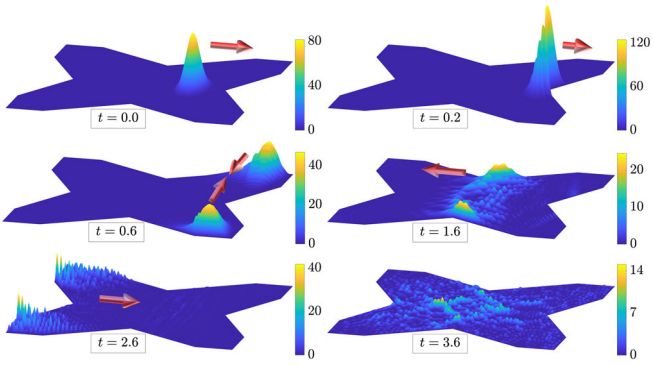

FIG. 2. An example of successive stages of the wave-packet evolution, $|\Psi(\mathbf{r}, t)|^2$, in the butterfly-shaped billiard. Red arrows indicate the directions of motion of the components. Initial velocity is aimed at the right inner corner.

We solve these four boundary-value problems for the Laplace operator numerically using the finite-element method and find eigenstates of each class up to a certain energy cutoff. The accuracy of the numerical solution decreases with the number of found eigenstates [22]. We use Weyl's law for the number of modes [23] to control it. Weyl's law sets the asymptotic behavior of the average number of eigenstates below energy $E = \hbar_{\rm eff}^2\varepsilon/2$ as: $\mathcal{N}(\varepsilon) \simeq [A/(4\pi)]\varepsilon - [P/(4\pi)]\sqrt{\varepsilon}$, $\varepsilon \to \infty$, where P is the billiard's perimeter. For our purposes, it is sufficient to use $N_{\rm max} \sim 10^4$ eigenstates, and within this range, we have a perfect agreement with Weyl's law, i.e., the number of found states is centered around the Weyl's asymptote. We repeat the calculations with the boundary-integral method and obtain the same results.

Along with this billiard, we introduce an effective mathematical billiard (Fig. 1, inner blue shape) obtained by tracing the set of positions available to the center of a circular particle of radius $\sigma\sqrt{\hbar_{\rm eff}/2}$ inside the polygonal billiard. The squeezing parameter σ is defined in Eq. (1).

Diagnostic tool.—To explore quantum dynamics, we use the OTOC [11–16] defined as

$$C(t) = -\langle[\hat{x}(t), \hat{p}_x(0)]^2\rangle, \tag{3}$$

where $\hat{x}(t)$ and $\hat{p}_x(t)$ are the Heisenberg operators of the x components of the particle's position and momentum. The OTOC probes the sensitivity of quasiclassical trajectories to initial conditions [10], as $\hat{p}_x(0) = -i\hbar_{\rm eff}\partial/\partial x(0)$, and hence $C(t) = \hbar^2\langle[\partial x(t)/\partial x(0)]^2\rangle$. Therefore, classical Lyapunov-like growth is anticipated at early times, $C(t) \propto \exp(2\tilde{\lambda}t)$, for a chaotic system, with $\tilde{\lambda}$ related to its Lyapunov exponent in the respective subspace.

As was shown in Ref. [16], whether the OTOC grows exponentially depends on an initial quantum state and the presence of a finite time window between the first collision and the Ehrenfest time. For billiards, a natural choice of the initial state is the minimal-uncertainty wave packet, Eq. (1). The Ehrenfest time in chaotic systems is short and grows logarithmically slowly with system size: $t_E = \ln(\hbar_{\rm eff}^{-1})/\lambda_{\rm cl}$, where $\lambda_{\rm cl}$ is the Lyapunov exponent of the classical counterpart [1]. This estimate is based on the fact that, in contrast to nonchaotic systems, the wave-packet spreading in chaotic systems is exponential. Extending the Ehrenfest window to cover the longtime ergodic classical behavior, which is required to define the global Lyapunov exponents in chaotic systems, is an exponentially demanding numerical task. However, local finite-time Lyapunov exponents can be defined, although they fluctuate at these short times [16].

Breakdown of classical-to-quantum correspondence.—In classically chaotic quantum billiards, the exponential growth of the OTOC may be related to the classical Lyapunov instability and extends up until $t \sim t_E$ [16]. At $t > t_E$, the wave packet is spread across the entire system, and no further exponential growth is possible. One can define the classical counterpart of the OTOC as follows:

$$C_{\rm cl}(t) = \langle\!\langle \lim_{\Delta x(0)\to 0} \left[\frac{\Delta x(t)}{\Delta x(0)}\right]^2 \rangle\!\rangle, \tag{4}$$

where $\langle\!\langle \cdots \rangle\!\rangle$ denotes the classical phase-space average over the Gaussian Wigner function corresponding to the initial quantum packet in Eq. (1), and Δx is the distance along the x axis between a pair of trajectories starting near some point in the phase space. $C_{\rm cl}(t)$ agrees with $C(t)/\hbar_{\rm eff}^2$ in chaotic systems all the way up to t_E. After that, $C(t)$ slows down and eventually saturates, while $C_{\rm cl}(t)$ continues to grow exponentially.

In the polygonal billiards, there are no positive classical Lyapunov exponents, and the corresponding classical OTOC does not grow exponentially at any time, as shown in the inset in Fig. 3 for the case of the butterfly-shaped polygonal billiard. However the quantum-mechanical OTOC in polygonal billiards shows a clear exponential growth at early times that has no origin in the classical counterparts, as demonstrated in Figs. 3 and 4.

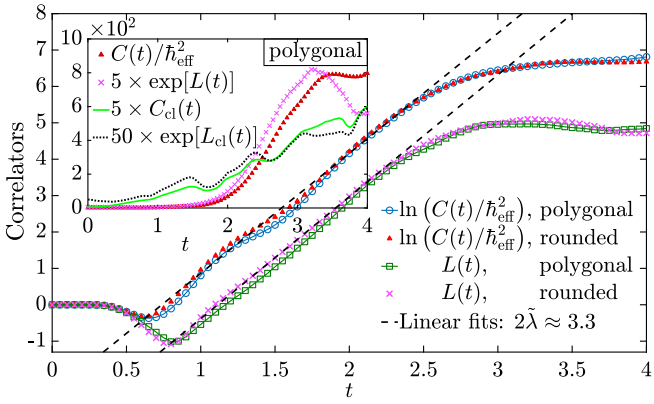

FIG. 3. *Main plot.* Open blue circles and line: logarithm of the OTOC in the butterfly-shaped billiard: $\ln[C(t)/\hbar_{\rm eff}^2] = \ln[-(1/\hbar_{\rm eff}^2)\langle[\hat{x}(t), \hat{p}_x(0)]^2\rangle]$. Solid red triangles: the same in the rounded version of this billiard. A remarkable agreement supports our finite-size smearing arguments. In addition, we show the corresponding behavior of an alternative diagnostic, $L(t) = \langle\ln(-(1/\hbar_{\rm eff}^2)[\hat{x}(t), \hat{p}_x(0)]^2)\rangle$, that swaps the order of averaging and logarithm to that in the proper definition of the classical Lyapunov exponent. For chaotic systems, one would expect $L(t) = 2\tilde{\lambda}t + \text{const}$ at $t < t_E$. Green squares and line: $L(t)$ in the polygonal butterfly-shaped billiard. Pink crosses: $L(t)$ in the rounded billiard. Dashed black lines: linear fits for $\ln[C(t)/\hbar_{\rm eff}^2]$ and $L(t)$ in the polygon. Both show the exponent $2\tilde{\lambda} \approx 3.3$ that is five times larger than the inverse time window, which ensures the validity of the fit. *Inset.* The comparison between $C(t)/\hbar_{\rm eff}^2$ and $C_{\rm cl}(t)$ [see Eq. (4)] and between $\exp[L(t)]$ and $\exp[L_{\rm cl}(t)] = \exp\{\langle\!\langle \ln[\partial x(t)/\partial x(0)]^2\rangle\!\rangle\}$ in the polygonal quantum and classical billiards, respectively. $\hbar_{\rm eff} = 2^{-7}$, $\sigma = 1/\sqrt{2}$, $R_s = (\sqrt{2} - 1/16\sqrt{2}) \approx 0.02$.

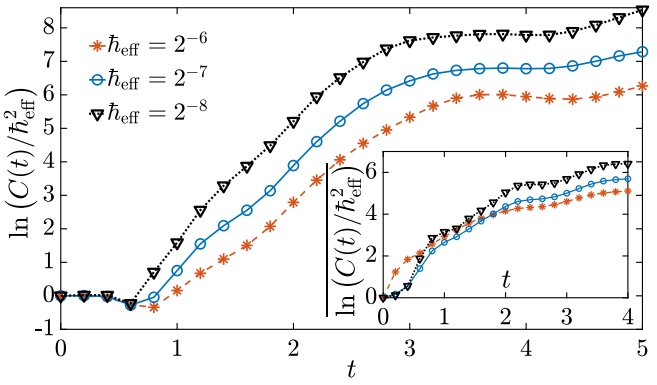

FIG. 4. *Main plot.* Logarithm of the OTOC in the butterfly-shaped billiard at three different values of $\hbar_{\rm eff}$. The exponential growth hinges on the finite wave-packet size. *Inset.* Logarithm of the OTOC in the quadrilateral billiard (Fig. 5), averaged over an ensemble of initial conditions as indicated by the bar, $\bar{\cdots}$, at the same values of $\hbar_{\rm eff}$.$\sigma = 1/\sqrt{2}$.

As discussed in the introduction, the motion of a minimal-uncertainty wave packet is similar to that of a finite-size disk. Classical motion of such a disk gives rise to an effective billiard that hosts a pointlike particle at the disk's center that is not allowed to approach the walls of the original billiard closer than by disk's radius. Many billiards preserve their status within the ergodic hierarchy upon this procedure (e.g., a stadium turns into a smaller stadium). Not so for nonconvex polygonal billiards. In such nonchaotic systems, there can still be measure-zero sets of unstable points, and these get smeared over finite-measure regions by introducing a finite size of the particle, which takes them up the ergodic hierarchy from the mixing to the K-chaotic class. A quantum wave packet can cause a similar effect.

In addition, polygons constitute an everywhere dense measure-zero set in the space of closed curves on a plane, and the phase space of the corresponding billiards contains isolated unstable points. A slight variation of the wall's shape almost always results in finite-curvature regions and smears out singular phase-space points. A possible consequence of that would manifest because, in contrast to a rigid disk, a quantum-mechanical wave packet effectively "rounds" singularities even if they originate from outer corners of polygons, including those in the convex polygonal billiards considered below. This can be generalized to a statement that quantum mechanics promotes measure-zero sets of unstable points into finite-measure sets. We check these conjectures by varying the billiard's boundary within the shaded gray region in Fig. 1, and, in particular, compare the behavior of the OTOC in the polygonal and in a rounded billiard, such as the middle red line in Fig 1. The latter system is classically chaotic. We find a good agreement between the quantum OTOCs in the two, as demonstrated in Fig. 3. In addition, from this comparison we can infer that there are no significant effects related to the nonsmoothness of the polygonal boundary, such as diffraction, as in the case in the quantum baker's map [24]. Note that the latter has a positive classical Lyapunov exponent, while in our case, the exponential growth of the OTOC appears to be a purely quantum effect.

We also point out here that in two early papers [25,26] one finds a discussion of the effect of finite perturbations in polygonal billiards and that this may lead to the appearance of exponential growth (classically and the corresponding signatures in quantum spectral properties). This may have the effect that the violation of the classical-to-quantum correspondence could find its alternative explanation in an improper choice of the classical counterpart (infinitesimal perturbations) and that considering finite perturbations could "heal" that apparent violation.

At smaller values of $\hbar_{\rm eff}$, the wave packets are tighter, and their sides are steeper. Following the reasoning in Ref. [27], it causes the rate of the OTOC's divergence, $\tilde{\lambda}$, to be larger than that at larger values of $\hbar_{\rm eff}$, as shown in Fig. 4, main plot. While the average Lyapunov exponent should go to zero in the limit of $\hbar_{\rm eff} \to 0$ in a polygonal billiard, averaging of the OTOC over a minimal-uncertainty wave packet whose trajectory crosses an inner billiard corner emphasizes the vicinity of the unstable point, which is shrinking as $\hbar_{\rm eff} \to 0$. Its overall contribution to the classical Lyapunov exponent goes to zero, as it should, but the OTOC does not reflect it properly. This highlights one of the difficulties in interpreting the growth rate of the OTOC in the classical sense. The inset in Fig. 4 shows an analogous behavior for the quadrilateral billiard shown in Fig. 4.

Quantum dynamics in convex polygonal.—Classical convex polygonal billiards do not change their status within the ergodic hierarchy upon promoting their point-particle versions to those with finite-size particles. However, quantum mechanically, they still show a rapid initial growth of the OTOC (superimposed with an oscillatory behavior), as we demonstrate for an irrational triangular billiard obtained from the quadrilateral one in Fig. 5 by removing the vertex. The effective rate of growth is smaller than for the nonconvex billiard, but signs of instability are still present. As shown in Fig. 5, the early-time behavior has a period of what looks like a sharp growth, although it is modulated by the effects of collisions with the walls.

We believe that this growth of the OTOC in convex billiards is due to the fact that a quantum simulation cannot access the proper small distance and longtime limit where classical Lyapunov exponents are defined. This behavior of the OTOC is a property of the initial state rather than the system itself. If so, similar growth should be observable in integrable systems as well. We have considered the simplest—rectangular—"billiard" and indeed found that some signs of spurious $\hbar_{\rm eff}$-dependent growth can be detected. Of course, these periods of growth have no relation to chaos or the butterfly effect.

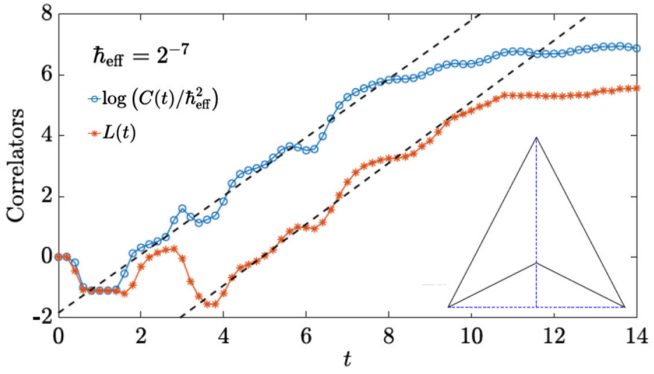

FIG. 5. Upper blue line and open circles: logarithm of the OTOC in an irrational triangular billiard (shown in the lower right corner). After an initial-condition-dependent delay, the OTOC shows exponential grows, although at a rate lower than that for the nonconvex billiard. Lower red line and asterisks: the L-correlator introduced in Fig. 3. Black dashed lines show linear fits with $2\tilde{\lambda} \approx 1$, which is over five times larger than the inverse growth time window, ensuring the validity of the fit.

All in all, there appear to exist two sources of rapid growth of OTOC in billiards: one related to a genuine Lyapunov instability (in chaotic billiards and those that are promoted in the chaotic hierarchy upon quantization) and a spurious growth related to a finite-size wave packet enforcing an "unfaithful" representation of the underlying classical dynamics. The latter spurious growth is present independently of the status of the effective billiard in the chaotic hierarchy. In order for the OTOC to have a physical meaning, it is important to disentangle these two contributions. The genuine Lyapunov growth, if any, can be extracted by examining scaling of the growth rate with $\hbar_{\rm eff}$ (the spurious growth should disappear in the true $\hbar_{\rm eff} \to 0$ limit, in contrast to quantum chaotic systems where it asymptotes a constant).

This research was supported by DOE-BES DE-SC0001911 (V. G. and E. R.) and NSF Grant No. DMS-160058 (L. B.). The authors acknowledge helpful discussions with Sriram Ganeshan, Arul Lakshminarayan, and Meenu Kumari and thank Colin Rylands for proofreading the manuscript. The authors are grateful to Centro Internacional de Ciencias (Cuernavaca, Morelos, Mexico), where this work was conceived, and personally to Thomas Seligman and Felix Izrailev for outstanding hospitality.

*Corresponding author.
efimroz@umd.edu

[1] G. P. Berman and G. M. Zaslavsky, Physica (Amsterdam) **91A**, 450 (1978); G. M. Zaslavsky, Phys. Rep. **80**, 157 (1981).
[2] M. Toda and K. Ikeda, Phys. Lett. **124A**, 165 (1987); Y. Gu, Phys. Lett. **149A**, 95 (1990); W. H. Zurek and J. P. Paz, Phys. Rev. Lett. **72**, 2508 (1994); Physica (Amsterdam) **83D**, 300 (1995).
[3] W. H. Zurek, Phys. Scr. **T76**, 186 (1998).
[4] M. Berry, in *Quantum Mechanics, Scientific Perspectives on Divine Action*, edited by R. J. Russell, P. Clayton, K. Wegter-McNelly, and J. Polkinghorne (CTNS/Vatican Observatory, 2001), pp. 41–54.
[5] W. H. Zurek and J. P. Paz, *Why we don't need quantum planetary dynamics: Decoherence and the correspondence principle for chaotic systems, in Epistemological and Experimental Perspectives on Quantum Physics*, edited by D. Greenberger, W. L. Reiter, and A. Zeilinger (Springer Netherlands, Dordrecht, 1999), pp. 167–177.
[6] M. Schlosshauer, Found. Phys. **38**, 796 (2008).
[7] N. Wiebe and L. E. Ballentine, Phys. Rev. A **72**, 022109 (2005); L. Ballentine, Found. Phys. **38**, 916 (2008).
[8] A. N. Zemlyakov and A. B. Katok, Mat. Zametki **18**, 291 (1975) [Math. Notes Acad. Sci. USSR **18**, 760 (1975)]; C. Boldrighini, M. Keane, and F. Marchetti, Ann. Probab. **6**, 532 (1978).
[9] M. Bolding, Topics in dynamics: First passage probabilities and chaotic properties of the physical wind-tree model, Ph. D. thesis, School of Mathematics, Georgia Institute of Technology, Atlanta, GA 30332, USA, 2018; L. A. Bunimovich, arXiv:1903.02634.
[10] A. I. Larkin and Yu. N. Ovchinnikov, Zh. Eksp. Teor. Fiz. **55**, 2262 (1969) [Sov. Phys. JETP **28**, 1200 (1969)].
[11] A. Kitaev, KITP talk, http://online.kitp.ucsb.edu/online/entangled15/kitaev/ (2014).
[12] J. Maldacena, S. H. Shenker, and D. Stanford, J. High Energy Phys. 08 (2016) 106.
[13] D. A. Roberts, D. Stanford, and L. Susskind, J. High Energy Phys. 03 (2015) 051; D. A. Roberts and B. Swingle, Phys. Rev. Lett. **117**, 091602 (2016); Y. Huang, Y.-L. Zhang, and X. Chen, Ann. Phys. (Amsterdam) **529**, 1600318 (2017); R. Fan, P. Zhang, H. Shen, and H. Zhai, Sci. Bull. **62**, 707 (2017); Y. Chen, arXiv:1608.02765; B. Swingle, G. Bentsen, M. Schleier-Smith, and P. Hayden, Phys. Rev. A **94**, 040302(R) (2016); B. Swingle and D. Chowdhury, Phys. Rev. B **95**, 060201(R) (2017); N. Y. Yao, F. Grusdt, B. Swingle, M. D. Lukin, D. M. Stamper-Kurn, J. E. Moore, and E. A. Demler, arXiv:1607.01801; M. Mezei and D. Stanford, J. High Energy Phys. 05 (2017) 065; S. V. Syzranov, A. V. Gorshkov, and V. M. Galitski, Ann. Phys. (Amsterdam) **405**, 1 (2019); V. Khemani, D. A. Huse, and A. Nahum, Phys. Rev. B **98**, 144304 (2018); S. Xu and B. Swingle, Nat. Phys. **16**, 199 (2020).
[14] E. B. Rozenbaum, S. Ganeshan, and V. Galitski, Phys. Rev. Lett. **118**, 086801 (2017).
[15] J. Chávez-Carlos, B. López-del-Carpio, M. A. Bastarrachea-Magnani, P. Stránský, S. Lerma-Hernández, L. F. Santos, and J. G. Hirsch, Phys. Rev. Lett. **122**, 024101 (2019).
[16] E. B. Rozenbaum, S. Ganeshan, and V. Galitski, Phys. Rev. B **100**, 035112 (2019).
[17] Y. G. Sinai, Russ. Math. Surv. **25**, 137 (1970).
[18] L. A. Bunimovich, Funct. Anal. Appl. **8**, 254 (1975); Commun. Math. Phys. **65**, 295 (1979).
[19] Y. G. Sinai, Introduction to Ergodic Theory, *Mathematical Notes (Book 18)* (Princeton University Press, Princeton, 1977).

[20] T. Araújo Lima, S. Rodríguez-Pérez, and F. M. de Aguiar, Phys. Rev. E **87**, 062902 (2013).
[21] G. Casati and T. Prosen, Phys. Rev. Lett. **83**, 4729 (1999).
[22] V. Heuveline, J. Comput. Phys. **184**, 321 (2003).
[23] H. P. Baltes and E. R. Hilf, *Spectra of Finite Systems* (Bibliographisches Institut, Mannheim, 1976).
[24] A. Lakshminarayan, Phys. Rev. E **99**, 012201 (2019).
[25] T. Cheon and T. D. Cohen, Phys. Rev. Lett. **62**, 2769 (1989).
[26] J. L. Vega, T. Uzer, and J. Ford, Phys. Rev. E **48**, 3414 (1993).
[27] T. Prosen, Phys. Rev. E **65**, 036208 (2002); T. Prosen and M. Žnidarič, New J. Phys. **5**, 109 (2003).